Non-linear Fowler-Nordheim plots in thin film polymer-fullerene composite devices (transition from hole-only to electron-only conduction)

Zivayi Chiguvare

University of the Witwatersrand, DST/Centre of Excellence in Strong Materials and Material Physics Research Institute, School of Physics, Private Bag 3, Wits 2050, Johannesburg, South Africa

Zivayi.Chiguvare@wits.ac.za

Abstract. We studied charge injection and transport mechanisms in blends of poly(3-hexylthiophene) (P3HT) and [6,6]-phenyl C61-butyric acid methylester (PCBM), by analyzing dark, temperature dependent current-voltage characteristics of the P3HT:PCBM blend thin films sandwiched between aluminium electrodes in a MIM configuration. We present a general method of interpreting Fowler - Nordheim plots of metal/semiconductor/metal devices with pronounced non-linear characteristics by dividing them into several regions based on physical origins. We show that by applying appropriate electric fields it is possible to switch from electron-only conduction to hole-only conduction in a single Al/P3HT:PCBM/Al device. We affirm that electrons can be selectively transported through the lowest unoccupied molecular orbital of PCBM at low applied voltages and low temperatures; and alternatively holes can be transported through the highest occupied molecular orbital of P3HT at higher applied voltages and high temperature, within a single device.

1. Introduction

Thin films of polymer- fullerene blends are interesting because electronic devices such as light emitting diodes, field effect transistors, and solar cells made using them can be flexible, light-weight, and far cheaper as compared to those based on inorganic materials such as silicon, or germanium. For instance the efficiency of solar cells based on P3HT:PCBM blends has risen from less than 1% in the early 1990's to above 5 % in 2009, prompting companies like Konarka[§] to start commercial manufacture of organic photovoltaic cells for consumer products with up to 1GW capacity per annum envisaged. The Physics underlying charge carrier injection and transport in such devices is however still not yet fully understood.

Charge injection in MIM (e.g. polymer) devices takes place by thermionic emission from metal electrode to some transport level in the polymer, and by quantum mechanical tunneling of charge carriers at high enough applied electrical fields. Charge transport is however determined by the characteristics of the bulk material itself, such as mobility and density of charge carriers, and the existence of impurities. The essential assumption of the Richardson-Schottky (RS) model of thermionic emission is that an electron from the metal can be injected once it has acquired sufficient thermal energy to cross the potential maximum that results from the superposition of the external and the image charge potential. For low bias the number of injected carriers is smaller or comparable to the

thermally generated intrinsic charge carriers, and the current – voltage characteristics can be described by Ohm's law:

$$J_{Ohm} = q(n_p \mu_p + n_e \mu_e) \frac{V}{d}$$

(1)

In the absence of traps, or when all traps are filled, J has a quadratic dependence on V, and follows the Mott-Gurney law:

$$J_{TFSCLC} = \frac{8}{9} \mu_p N_v \varepsilon \varepsilon_0 \frac{V^2}{d^3}$$

(2)

Fowler–Nordheim tunneling is the wave- mechanical tunneling of an electron through an exact or rounded triangular barrier. The F-N model for tunneling injection ignores image charge effects and invokes tunneling of electrons from the metal through a triangular barrier into unbound continuum states. It predicts:

$$J_{FN}(F) = \frac{q^3}{16\pi^2 \hbar \phi} F^2 \exp\left[-\frac{4(2m_{eff})^{1/2} \cdot \phi^{3/2}}{3\hbar e F} \right]$$

(3)

independent of temperature. Here m_{eff} is the effective mass of the carrier inside the dielectric.

Observation of straight line fits of $J(V)$ data in F-N plots is usually taken as confirmation that quantum mechanical tunneling of charge carriers dominates the conduction mechanisms of a given single carrier device. The physical origin of nonlinearity in the Fowler–Nordheim plot is still a debatable issue. Non-linear F-N curves were observed by several authors [1, 2], where the F-N plot is curved downwards for low applied fields, with positive slope, and upwards at high fields with negative slope, and approaching the sought after straight line approximation [3]. Various reasons have been suggested for the occurrence of the first inflexion point: F-N plot curvature can be relatively small [4], so where marked curvature occurs in experimental plots, usually some other effect must be operating, such as the presence of vacuum space charge, electron supply limitation inside the emitter, or statistical effects associated with a many emission- sites electron source [5]. We have shown that the first inflexion point leading to the appearance of the first minimum is due to the transition from conduction by thermionically injected charge carriers to conduction by field emission injected charge carriers, the sum of which gives a single minimum in a F-N plot [6]. Both F-N electron and hole tunneling [7] have been observed in experiments.

We note that a second inflexion point at higher fields is evident in the experimental results of several studies [8, 9], but the authors have not referred to it, limiting their discussion to the straight line approximation. A flattening of the F-N plots, linked to the second inflexion point, was suggested to be due to several factors such as a finite reflection coefficient, a finite energy width of emitted electrons, and space charge effects [10]. We have observed even a third inflexion point as applied electric field is increased and will elucidate the physical origins of the observed non-linearities in this paper. Such behaviour was referred to as oscillatory behaviour of the F-N plots, by Khlifi et al. [11] who analysed more than 3 inflexion points and attributed the oscillations to some 'excess' current.

2. Materials and Methods
Glass substrates were cleaned in deionized water, acetone, toluene and isopropanol, respectively, in a hot ultrasonic bath. The Al electrode in contact with the glass substrate was deposited by thermal evaporation in better than 5×10^{-7} mbar vacuum. A chloroform-toluene based 1:2 polymer – fullerene blend by mass solution (10 mg/ml) was then spin-coated in the nitrogen atmosphere of a glove box, O_2 – 2 ppm and H_2O – 0.01 ppm giving films of thicknesses around 80 nm. The aluminium top electrodes were deposited by thermal evaporation in high vacuum, better than 5×10^{-7} mbar at ~ 0.2 nm/s rate.

Note that the Al electrodes are each in contact with both P3HT and PCBM. All devices were stored in nitrogen atmosphere prior to measurement. The formulae of P3HT and PCBM, and energy level diagrams of the studied Al/P3HT:PCBM/Al devices (under non – equilibrium conditions) are shown in Fig. 1. All devices were heated slowly up to 380 K before measurement was initiated.

3. Results

Typical current-voltage characteristics of Al/P3HT:PCBM/Al thin film devices are shown in Fig. 2. The Al/P3HT:PCBM/Al devices are electron only devices at low applied electric fields. At temperatures above absolute zero, electron-hole pairs are generated by thermal excitation resulting in electrons in the LUMO of P3HT, and holes in its HOMO. The electrons are immediately transferred to LUMO PCBM through an ultrafast charge transfer ($\sim 10^{-15}$ s). The resulting quasi stable state is that of positive P3HT radicals in the vicinity of negative PCBM radicals, where electron-hole recombination is inhibited by potential barriers at heterojunctions distributed within the bulk. Such a configuration favours the transport of electrons through the LUMO of the PCBM, while holes are transported through the HOMO of the P3HT.
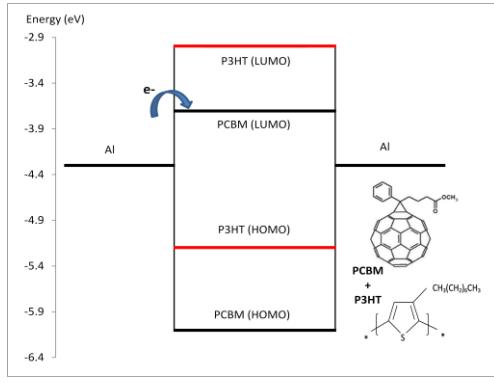
Fig. 1 Energy band diagram of an Al/P3HT:PCBM/Al device. The inset shows the chemical formulae of the materials making up the composite layer.
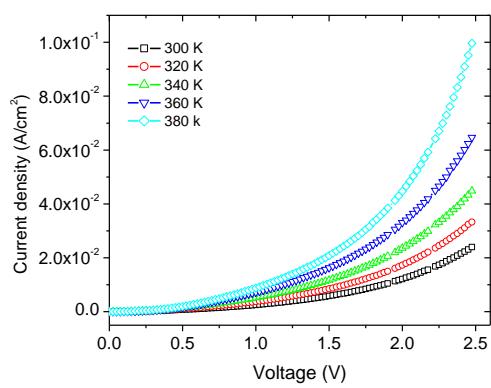
Fig. 2 Typical current voltage characteristics of an Al/P3HT:PCBM/Al device in linear scale.

Double log plots of *J(V)* characteristics show that ohmic and trap free SCLC (TFSCLC)analysis alone cannot describe completely the behaviour of these devices. The curves of Fig. 3 do not exhibit the slope ~ 1 region even at the lowest applied voltages. Such behaviour indicates that even at low voltages, there is some significant injection of charge carriers from the electrodes; in this case, electrons are injected from the Al electrode into the LUMO of PCBM. The slopes are constant between 1 and 2, suggesting a mixture of ohmic and space limited currents at these low voltages. Slopes increase beyond 2, but the lines have an oscillatory nature and are not straight as would be expected for SCLC conduction in the trap filling regime. Clearly TFSCLC cannot adequately describe the conduction mechanism in these Al/P3HT:PCBM/Al devices.

We investigate the charge injection mechanisms and their contribution to the total measured current, and observe non-linear F-N curves as indicated in Fig. 4. Each F-N curve has variable positive slope at low applied electric fields, which changes sense and becomes negative close to the highest applied fields, for lower temperatures. At intermediate applied voltages, the F-N curves have negative slopes, which again change to positive and finally

straight line regions of negative slopes are observed as voltage is increased further. Thus three inflexion points resulting in two minima are observed in the F-N curves.
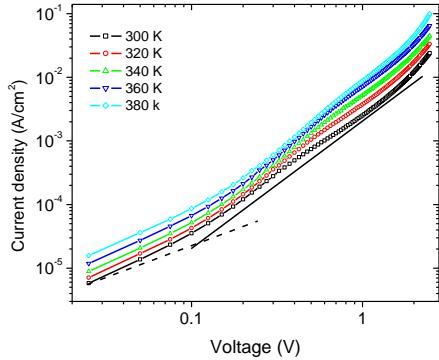
Fig. 3 Double log plot of *JV* curves for Al/P3HT: PCBM/Al devices. Dashed lines indicate slope = 1, and dotted lines indicate slope = 2
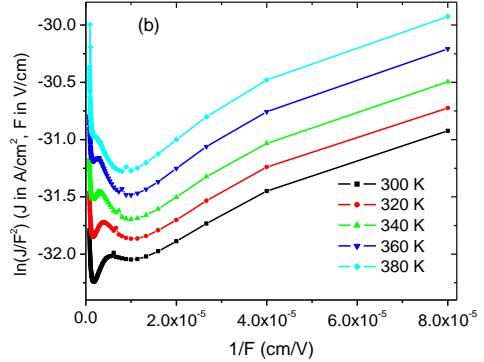
Fig. 4 Fowler Nordheim tunneling curves for Al/P3HT:PCBM/Al devices

Two negative slope regions with straight line tendencies are clearly observed; suggesting two tunnelling regimes in these devices (see Fig. 5). We argue that the first minimum as we increase voltage is due to significant tunnelling of electrons from Al electrode into the LUMO of the PCBM. In a single carrier device, straight lines should then be observed and characteristics of the tunnelling barrier studied. However, a second point of inflexion again changes the slope to positive, suggesting a reduction in the rate of increase of charge carriers available for current conduction. This can only happen if some of the injected charge carriers are not reaching the opposite electrode. We attribute this to recombination of charge carriers within the bulk of the film

The opposite electrode also injects charge carriers (holes) into the HOMO of P3HT, thereby shifting the recombination plane from the positive electrode towards the negative electrode. This is illustrated in Fig. 6 where a typical energy diagram of a MIM device with symmetric electrodes, under non-equilibrium conditions is shown; hole injection barrier φ_2 is greater than electron injection barrier φ_1; (b) Small negative bias on *metal 1* modifies the energy band structure, and both electrons and holes can be injected by thermionic emission over the trapezoidal barriers. The effective thickness traversed by charge carriers is the same as the film thickness and tunnelling is negligible; (c) At intermediate applied voltages, the effective thickness for electron conduction is smaller than the device thickness, and the electrode of smaller injection barrier φ_1, injects holes significantly by F-N tunnelling (electron-only device); (d) At high V_a both barriers are now smaller than qV_a, and tunneling injection takes place from both electrodes, leading to ambipolar conduction. As the voltage is further increased the injection of holes becomes so significant that the recombination plane is shifted until it reaches the negative electrode, in which case current conduction through the film is now due to holes through HOMO of P3HTonly. The straight line region can then be used to study the hole injection barrier at the Al/P3HT interface.

4. Model
We note that the first point of inflexion originally suggested to being the transition from direct to F-N tunnelling [12] is rather due to changeover, from thermionic emission dominated

injection, to FN tunneling dominated injection, of electrons across the Al/PCBM LUMO barrier.
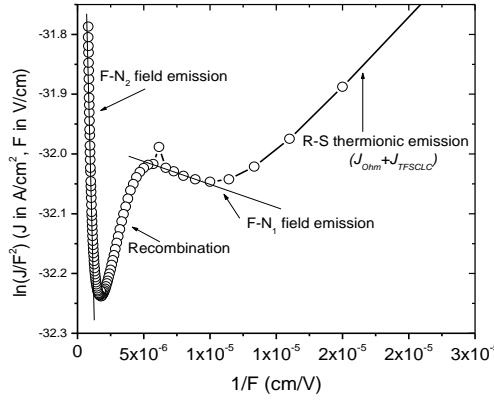
Fig. 5: 300 K F-N plot for Al/P3HT:PCBM/Al device, showing the four different regimes: R-S thermionic emission, electron tunneling through the lower barrier electrode, recombination regime, and hole tunneling through higher barrier electrode.
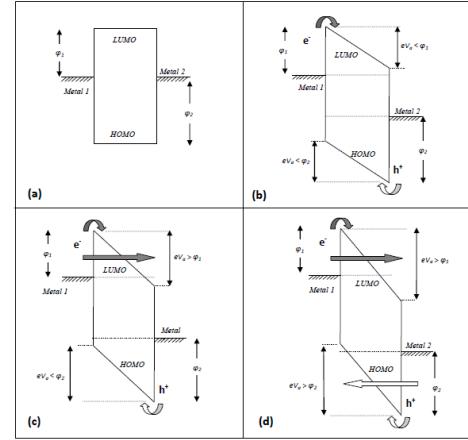
Fig. 6: Typical energy diagram of a MIM device with symmetric electrodes, **(a)** under non-equilibrium conditions; (b) under low bias; (c) under intermediate bias; and (d) under high bias.

We propose that the total current in the studied devices can be modelled as:

$$J_{tot} = J_{TE} + J_{FE} - J_{rec}, \tag{4}$$

Where J_{TE} is the current due to thermionically emitted charges, J_{FE} is the current due to tunneling injection, and J_{rec} is the current due to charge carrier recombination.

$$J_{tot} = J_{Ohm} + J_{SCLC} + J_{FN1} + J_{FN2} - J_{rec} \tag{5}$$

We propose a recombination current of the form:

$$J_{rec} = \alpha \frac{J_{FN1} \cdot J_{FN2}}{(J_{FN1} + J_{FN2})}, \tag{6}$$

where α is a temperature dependent constant associated with the position of the recombination plane. The value of α is minimal at the electrodes, $\alpha = 0$, but can take values greater than 1 becoming maximum at a plane where $\mu_p n_p = \mu_e n_e$. The recombination current cannot be measured by an ammeter because the injected charges never reach the electrodes. Instead they annihilate each other resulting in the emission of a photon, or of a phonon, which may be absorbed by the lattice, increasing the temperature of the device. We have employed Eqs. (5) and (6) in an in-house developed MATLAB programme to fit our data and obtained reasonable fits as indicated in Fig. 7.

In Fig. 8 we illustrate the effect of varying the recombination constant α while keeping all other factors constant. For high α we obtain a recombination regime for a larger span of applied fields, while this becomes smaller when α is reduced. At $\alpha = 0$, the recombination regime is not observed at all, and an apparent smooth transition from electron only to hole only conduction should be observed. In this case it can be difficult to determine the two slopes due to F-N tunneling.
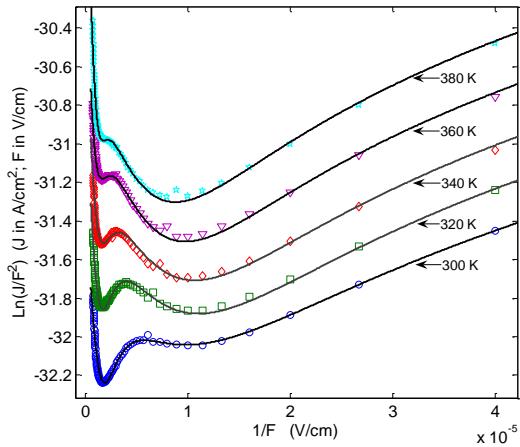
Fig. 7: Model fits to data.
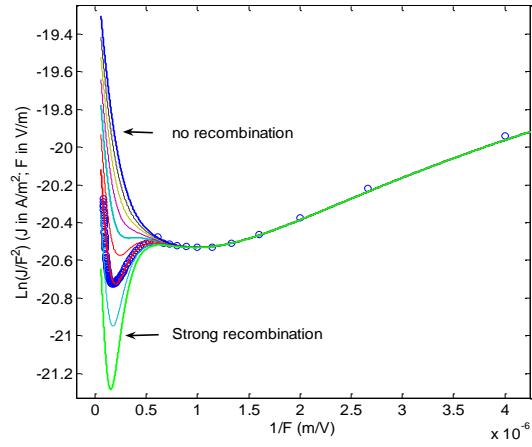
Fig.8: The slope of the FN curves for tunneling injection through lower barrier electrode is influenced by the recombination strength.

This slope cannot be used to estimate the electron tunneling barrier height, but on the contrary the tunneling regime at the higher barrier electrode is constant for all temperatures. If sufficiently high fields were applied, then the straight line observed would be attributed to hole tunneling in this case. It is therefore reasonable to expect that both n and μ increase with temperature for our Al/P3HT:PCBM/Al thin film devices (see Fig. 7).

5. Conclusions

We conclude that the nonlinearity in the FN plots originates from the transition from TE at low field to FE at moderately high electric fields(first minimum); from the transition from single to ambipolar conductivity (also associated with significant recombination) at sufficiently high fields (first maximum); and finally from the transition from ambipolar to single carrier conductivity of the opposite charge carrier of opposite sign (second minimum) after which the recombination plane shifts completely to the opposite electrode.

References
[1] C. Lee, J.Y. Park, Y.W. Park, Y.H. Ahn D. S. Kim, D.H. Hwang, T. H. Zyung, J. Kor. Phys. Soc. **35**, S291 (1999).
[2] A.J. Heeger, I.D. Parker, Y. Yang, Synth. Met. **67**, 23-29 (1994).
[3] S. H. Choi, B. Kim, C. D. Frisbie, *Science* **320**, 1482 (2008).
[4] C. J. Edgcombe, and N. de Jonge, J. Vac. Sci. Technol. B **24**, 869 (2006).
[5] R. G. Forbes, and J. H. B. Deane, Proc. R. Soc. A, **463**, 2907 (2007).
[6] Z. Chiguvare, J. Parisi, V. Dyakonov, J. Appl. Phys. **94**, 2440 (2003).
[7] R. K. Chanana, K. McDonald, M. Di Ventra, S. T. Pantelides, and L. C. Feldman, G. Y. Chung, C. C. Tin, and J. R. Williams, R. A. Weller, Appl. Phys. Lett., **77**, 16 (2000).
[8] C. Lee, J.Y. Park, Y.W. Park, Y.H. Ahn D. S. Kim, D.H. Hwang, T. H. Zyung, J. Kor. Phys. Soc. **35**, S291 (1999).
[9] G. Lai, Z. Li, L.Cheng, and J. Peng, J. Mater. Sci. Technol., **22**, 677 (2006).
[10] Y. Gohda, Y. Nakamura, K. Watanabe, and S. Watanabe, Phys. Rev. Lett. **85**, 1750 (2000).
[11] Y. Khlifi, K. Kassmi, L. Roubi, and R. Maimouni, Phys. Stat. Sol. (A) **182**, 737 (2000).
[12] J. M. Bebee, B. S. Kim, J. W. Gadzuk, C. D. Frisbie, and J. G. Kushmerick, Phys. Rev. Lett. **97**, 026801 (2006).

---

§ http://www.konarka.com